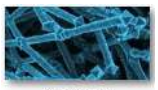
Materiales

Revista Mexicana de Ingeniería Química

Vol. 13, No. 3 (2014) 887-896

STUDY OF CONSTRAINED SINTERING OF POWERS USED TO CRACKS REPARATION

ESTUDIO DEL SINTERIZADO RESTRINGIDO DE POLVOS UTILIZADO PARA REPARACIÓN DE FISURAS

L. Olmos[1]*, A.M. Estrada-Murillo[2], J. Lemus-Ruiz[2], R. Huirache-Acuña[3], H.J. Vergara-Hernández[4], P. Garnica-González[4], and J.M. Salgado[5]

[1]*Coordinación de la Investigación Científica,* [2]*Instituto de Investigaciones Metalúrgicas,* [3]*Facultad de Ingeniería Química, Universidad Michoacana de San Nicolás de Hidalgo, Morelia, México.*
[4]*Posgrado de Ciencias en Metalurgia, Instituto Tecnológico de Morelia, México.*
[5]*Centro de Ingeniería y desarrollo Industrial. Santiago de Querétaro, Querétaro, México.*

Received May 28, 2013; Accepted July 31, 2014

Abstract

Sintering is a thermal treatment normally used to produce parts from different types of powders, and it is a phenomenon that has been studied since the 1950's. Mechanisms and diffusion paths for several materials have already been established. However, the use of sintering powders to repair fissures on solid materials has rarely been studied. The aim of this work is to study the solid state sintering of copper powders filling artificial grooves in a bar of solid copper. Sintering was carried out in an electrical furnace under H_2 and Ar (10-90 respectively) atmosphere at two different temperatures, 1000 and 1050ºC. The powder used to fill the grooves was a spherical atomized copper powder with a wide particle size distribution, 0-63 μm. Sintering of particles was evaluated at the edge of the solid bar and at the center of the groove by scanning electron microscopy (SEM). It was observed that particles sintered well on the wall's surface at the site of the artificial groove. Greater densification reached by the smaller particles and higher sintering temperatures creates defects inside the groove. Those defects are the consequence of the constraints of sintering, and the necks developed during the thermal cycle could be broken by the higher stresses generated during densification.

Keywords: constrained sintering, copper, solid state sintering, defects evolution, cracks healing.

Resumen

El sinterizado libre es un tratamiento térmico usado para fabricar partes sólidas a partir de diferentes tipos de polvos. Este fenómeno se ha estudiado desde los años 50 y los mecanismos de difusión para diversos materiales son conocidos. Sin embargo, el sinterizado restringido ha recibido poca atención, a pesar de las aplicaciones que puede tener como la reparación de fisuras en materiales que no pueden ser soldados. El objetivo de este trabajo es estudiar el sinterizado restringido de polvos de cobre depositados al interior de una ranura creada artificialmente en barras sólidas de cobre. Se evaluó el efecto del tamaño de partícula y de la temperatura de sinterizado sobre la evolución microestructural. El sinterizado se llevó a cabo en un horno eléctrico a dos temperaturas, 1000 y 1500°C, bajo una atmosfera reductora de una mezcla de H_2 y Ar (10-90 respectivamente). Los polvos usados son esféricos y con dos distribuciones de tamaño de partícula, 0-40 y 40-63 μm. La evolución del sinterizado fue evaluada al borde de la barra sólida y al centro de la ranura mediante microscopia electrónica de barrido. Los resultados muestran que el método es capaz de reparar fisuras y que los contactos entre partículas y las paredes se desarrollan de manera satisfactoria. Sin embargo, se encontró que altas densificaciones generan esfuerzos suficientemente fuertes para romper los contactos creados entre partícula-pared y también entre partícula-partícula, generando defectos como grietas o delaminaciones al borde de la pared. Se encontró que el uso de partículas de menor tamaño es más perjudicial para la unión entre partículas y pared.

Palabras clave: sinterizado restringido, cobre, sinterizado en estado sólido, evolución de defectos, reparación de fisuras.

*Corresponding author. *E-mail*: luisra24@gmail.com

1 Introduction

Solid state sintering is the final step to produce parts by the metallurgical powder technique that is used to fabricate composites (Subrata and Partha, 2011), nanomaterials (Khalil and Abdulhakim), porous materials (Wei *et al*, 2012) and monolithic bulk materials for different industries (Panigrahi *et al*, 2005; Showaiter and Youseffi, 2008). This phenomenon has been studied extensively by different authors (Kingery and Berg, 1955; Kuczynski, 1949; Frenkel, 1945; German, 1978; Exner, 1979; Coble, 1958). Models describing the evolution of the microstructure during sintering are based on the two spherical particles assumption (Pan *et al*, 1998; Parhami and McMeeking, 1998), and numerical simulations of sintering were performed from two spheres model (Ch'ng and Pan, 2007; Mori *et al*, 1998) to the most recent discrete element method (DEM) (Martin *et al*, 2006; Henrich *et al*, 2007; Olmos *et al*, 2009) and Monte Carlo numerical codes (Mori *et al*, 2004; Tikare *et al*, 2006). Exner *et al*. pointed out that large pores could be grown because of the particles' rearrangement, which is not taken into account for the two sphere model (Exner and Petzow, 2006). Recently, with the aid of novel characterization techniques like X ray microtomography, the evolution of the microstructure during sintering has been followed by in-situ experiments, in particular for spherical copper particles (Lame *et al*, 2004; Vagnon *et al*, 2008; Olmos *et al*, 2009). From the analysis of the 3D images, qualitative and quantitative data were obtained, and the rearrangement of particles and the collective phenomena occurring during a whole sintering cycle were measured. Data from the microtomography experiments were used to validate and improve simulation codes based on the discrete element method (Olmos *et al*, 2009). Results showed that sintering of different size of particles could be well represented by an equivalent radius. Nevertheless, sintering on the solid substrate has received less attention; just a few simulation experiments have been performed in that area (Scherer and Garino, 1985; Hsueh 1985; Martin and Bordia, 2009; Rasp *et al*, 2012). The evolution of defects in the granular part was pointed out to be the main challenge to overcome in order to manufacture films and Bi-materials. As the understanding of the fundamentals of sintering improves, the process could be used to accomplish different tasks.

Materials suffering cracks while experiencing high stress under working conditions that stretching them to the limit of their capabilities is one of the most frequent problems in the industry. In order to repair those cracks, the welding process is often used. However, welding is not appropriate for complicated alloys, ceramics or composite materials because the zone close to the cracks suffers changes in the microstructure due to the higher temperatures attained by this method. This could be detrimental for the mechanical properties of the material, particularly for complex materials. In this case, sintering of powders could offer a new alternative to repair cracks using powders with the same composition as the bulk material because the solid state sintering is carried out at temperatures under the melting point. It was shown that the sintering temperature could be notably reduced using smaller particles (Anselmi-Tamburini *et al*, 2006), which would be helpful to keep and to control the microstructure of the solid material. Nevertheless, it is necessary to study the behavior of sintering under constrained conditions like the schema of a crack, where the crack's wall will surround the powders.

This work has as its main objective to investigate the behavior of the sintering of copper powders introduced into an artificial groove. We chose copper as the model material because the sintering of powders does not present allotropic transformation, and also it has been deeply studied in the past, so we can focus the research on the effects of the constrained sintering into the grooves. Parameters like particle size distribution and sintering temperature will be studied in this paper to assess their effect on the process of cracking repair.

2 Experimental

The copper powders used are atomized spherical particles furnished by Ecka granules. The initial particle size distribution provided by the manufacturer contained particles smaller than 63 μm. Then the powders were separated using a sieve into two different distributions: the first one containing particles larger than 40 μm, and the second one having particles smaller than 40 μm. Powders were observed by scanning electron microscopy (SEM), and the spherical shape as well as the polycrystalline particles are shown in Figure 1a. Particle size distribution was calculated from several SEM pictures of the powder, and both particle size distributions are shown in Figure 1b.

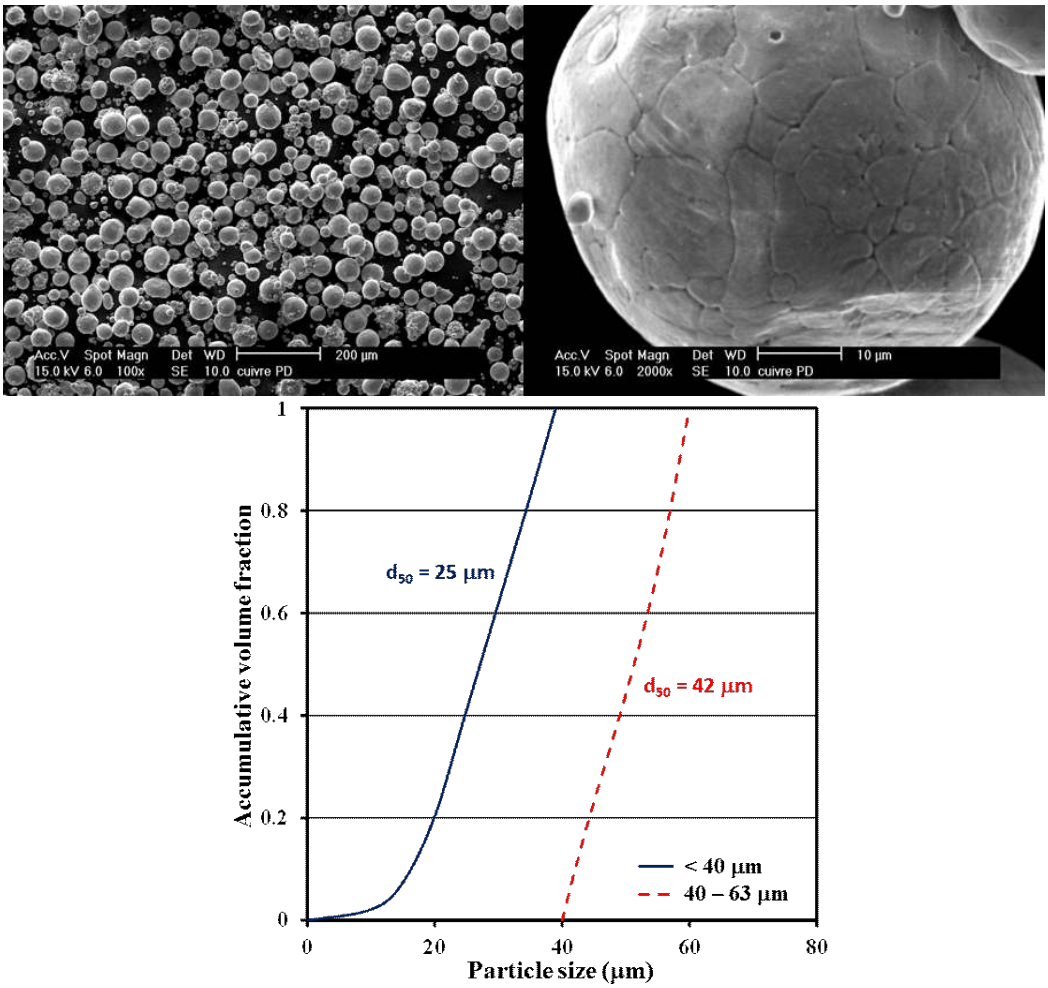

Fig. 1. The copper powders' characteristics, (a) shape of particles and (b) particle size distribution.

In the case of the smaller powders, a broad particle size distribution with an average size of particle of 25 μm was observed. In the second case, more than 80% of the particles were between 40 and 45 μm, and the average particle volume was 42 μm.

Solid copper bars were cut in rectangle shapes of 5 cm long and 8 mm wide and 8 mm high. Then samples were milled in the center with a 2 mm mill to a depth of 5 mm, as shown in Figure 2.

After that, solid bars were introduced into a bath of alcohol which was ultrasonically stirred for 5 minutes in order to clean the surface that would be in contact with the powders. Finally, the powders were poured into the groove using a funnel with a 1 mm diameter until it was completely full with powders. Then the samples were tapped and the free space into the groove leave for the rearrangement of particles was refilled with powders again. Finally the upper surface was swept with a plane plate with the objective being to remove the powders from the surface, and to get a smooth surface at the same level.

Sintering of the samples was performed in an electrical furnace at two different temperatures between 1000 and 1050°C through heating up at 25°C/min in a reducing atmosphere (with a mixture of Argon and 10% of Hydrogen) to prevent oxidation of the copper particles and bars. The duration of the sintering plateau was one hour. That time was assessed from dilatometric tests performed with the loose powders simply poured into an alumina crucible then they were tapped before to introduce them to the dilatometer.

The samples were cut in a perpendicular direction to the crack, and then they were polished by using silicon carbide paper with different sized grains that varied from coarser to finer.

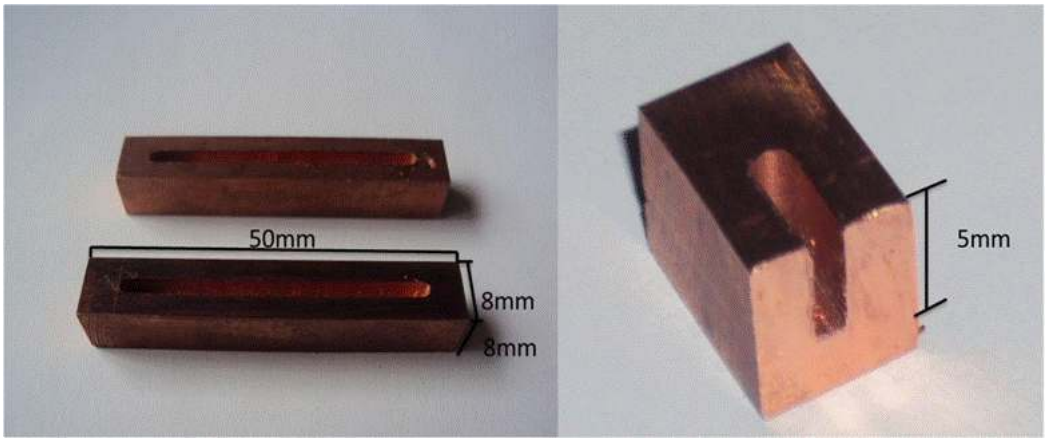

Fig. 2. Copper solid bars with the artificial groove in the middle.

Then they were finally polished using diamond paste with 1 μm grain size. Evolution of the microstructure was observed by SEM, and the neck sizes were evaluated, for those created between particles in the middle of the sample and those created between particles and the walls.

3 Results and discussion

Figure 3a shows the axial shrinkage of loose powders during free sintering assessed by means of dilatometric tests for both 40-63 μm and under 40 μm particle size distributions during the whole thermal cycle, inside of the alumina crucible. It is observed a large swelling at 450°C which is due to the elimination of the oxygen contained inside the particles; this phenomenon has been explained before by other authors (Upadyaya *et al*, (1998); and Olmos *et al*, (2009); presented more details about this). It is notice that larger powders generate larger swelling that is because they have larger oxygen contents. After the swelling, shrinkage due to sintering starts around of 835°C for both samples, that continues until the end of sintering plateau. At the end a final shrinkage due to the cooling is observed. In Figure 3b, we depict the densification of samples after sintering was activated around of 835°C, it is observed that activation for the smaller powder (< 40 μm) occurred slightly earlier. The initial relative densities for larger particle sized powders were 0.65 and 0.64 for the smaller ones. Because of the thermal dilatation and the swelling experimented by atomized copper powders during the heating stage the relative densities at the beginning of the sintering (around 835°C) were lower than the initial ones 0.618 and 0.622, respectively. It was observed that the smaller powders sintered faster than the larger ones. However, densification of the smaller particles was only 16% greater than the larger ones during the heating before reaching the sintering temperature. This value is negligibly compared to the one for the final densification during the sintering plateau where the densification was 200% larger for the smaller particles than for the larger ones. The behavior during the cooling was very similar for both cases. The final relative densities were 0.71 for the larger particles and 0.81 for the smaller ones. Those values of densification mean a reduction in volume of 9 and 26 percent, respectively, from the original volume occupied by the loose powders before sintering. This is an important fact to know because densification inside the groove will be constrained by the walls around the powders that will still be rigid without deformation, or densification.

Figures 4 and 5 show the inner surface of the sintered powders in the groove at 1000°C, for the larger and the smaller particle size distributions, respectively. In Figure 4a, it is observed that particles were well distributed in the groove. No defect of the groove's walls is noted, and the upper profile is nearly straight as Figure 4b confirms. The porosity observed is normal and classic to the free sintering of powders. Necks between the particles and the walls were developed as well as the particle-particle necks, as it is shown in Figures 4c and 4d.

Densification of sintered particles inside of the groove with the smaller particles was higher than for the larger particles when they were treated to the same thermal cycle, as we can see in Figures 5a and 5b. The reduction of the volume implies 100 μm from the top of the surface of the sample.

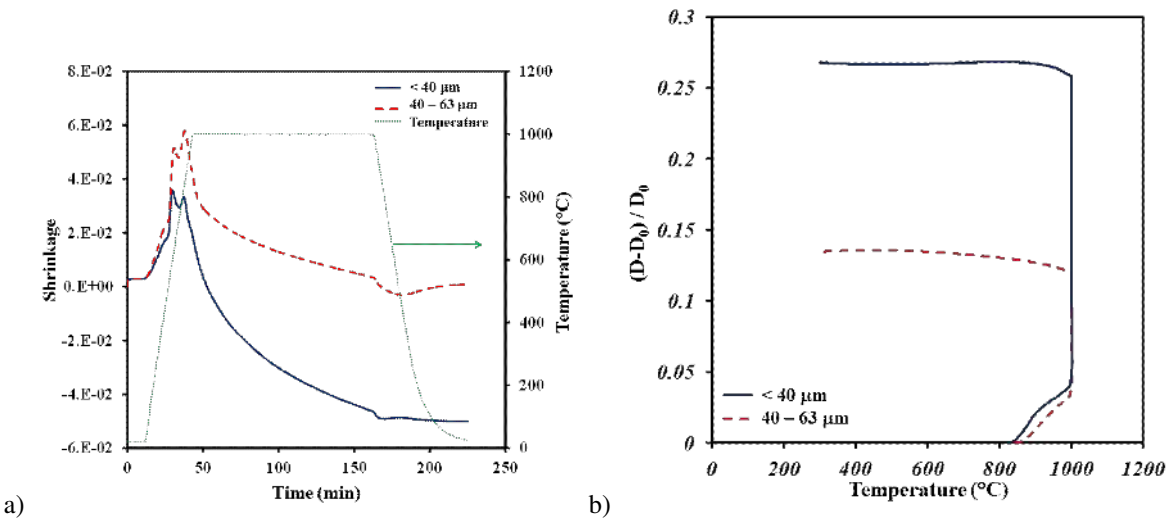

Fig. 3. Shrinkage (a) and densification (b) of the copper loose powders during sintering at 1000°C for 1h, solid line for 40-63 μm powders, and dashed line for < 40μm powders.

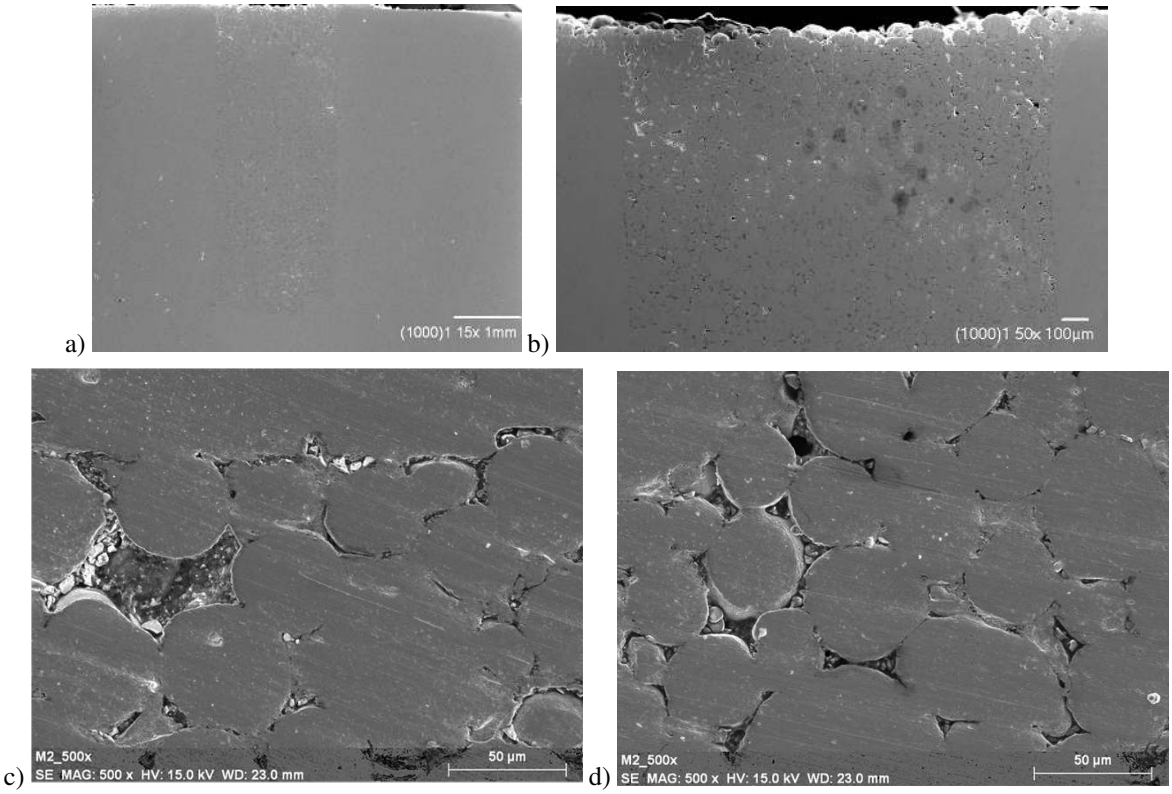

Fig. 4. Micrographs of the inner surface of the groove filled with larger particles (40-63 μm) after sintering at 1000°C, (a) whole groove surface, (b) upper profile, (c) sintered particles at the wall?s groove and (d) particles at the middle of the groove.

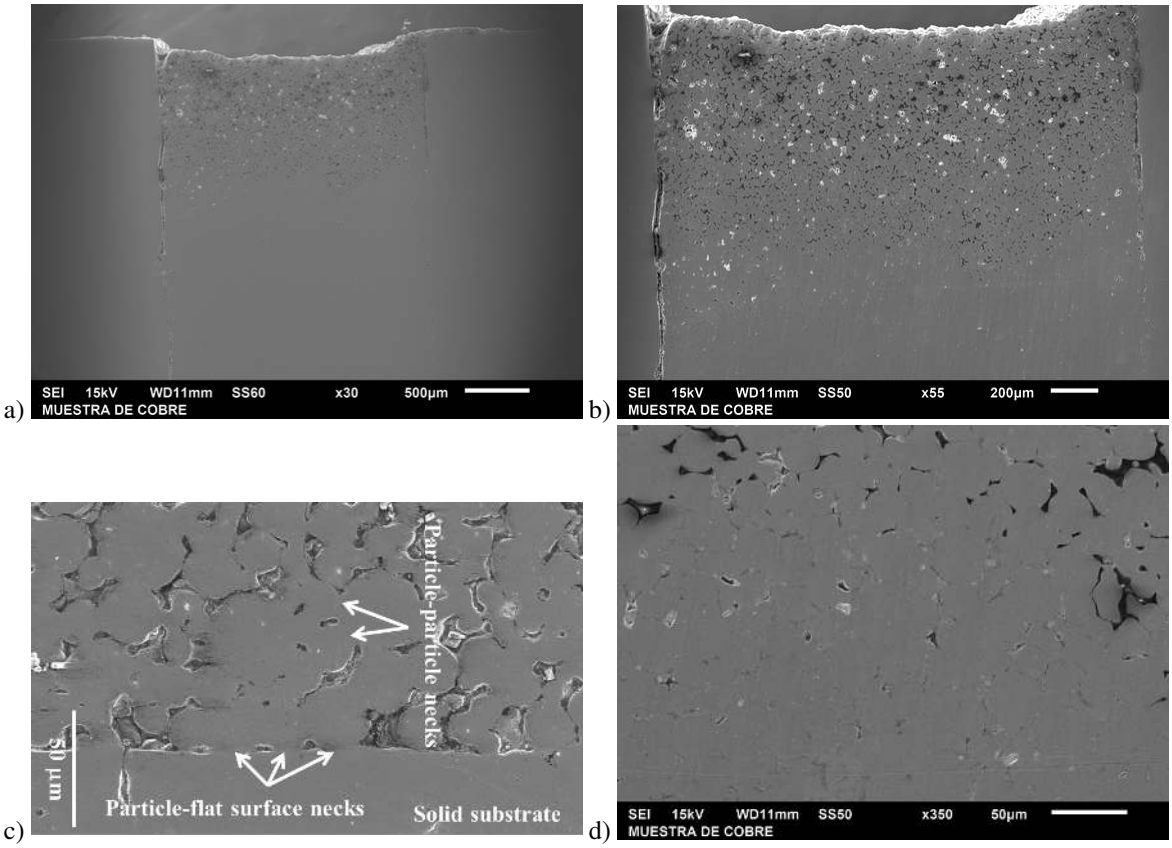

Fig. 5. Micrographs of the inner surface of the groove filled with smaller particles (< 40μm) after sintering at 1000°C, (a) whole groove surface, (b) upper profile, (c) sintered particles at the wall's groove and (d) particles at the middle of the groove.

That densification has generated delamination of particles from the walls close to the surface of the sample (Figure 5a). In spite of that, the profile at the upper surface seems to be flat, which might be caused by the delamination observed at the upper surfaces of the crack, as we can see in Figure 5b. The sintering between particles and the flat surface of the wall's groove was well developed, even better than it was for the larger particles, as shown in Figure 5c. On the other hand, at the center of the sample far from the wall, sintering between particles is achieved normally, it means that necks between particles are larger and the pores are smaller than those observed for the larger particles.

We observed that as the densification increased, the defects close to the walls appeared in particular for the smaller particles, so we decided to increase the sintering temperature up to 1050°C with the aim to observe the evolution and location of the defects created during the densification process. Figure 6 shows samples filled with the larger particles and sintered at 1050°C for one hour. We can observe defects appearing close to the walls at the upper surface, of the groove. In addition, in Figure 6a, we can see the beginning of larger pores growing inside the groove from the wall to the center of it. In spite of that, the sample's surface doesn't exhibit any change, it is flat as shown in Figure 6b, although a little shrinkage is observed when comparing to the upper boundary of the groove. The joint between particle-particle is stronger at this sintering temperature as it was expected, and neck sizes are larger between particles as well as at the contact particle-wall. In fact, none of the boundaries could be observed at the joint, as shown in Figures 6c and 6d. Fig. 7 shows the densification of the samples filled with the smaller particles when sintering was carried out at 1050°C. We found that it was higher when compared with samples of Fig. 6, as expected. At the upper surface a pronounce profile was created, and the shrinkage of the powders was approximately 400 μm from the surface of the groove, as noted in Figs. 7a and 7b.

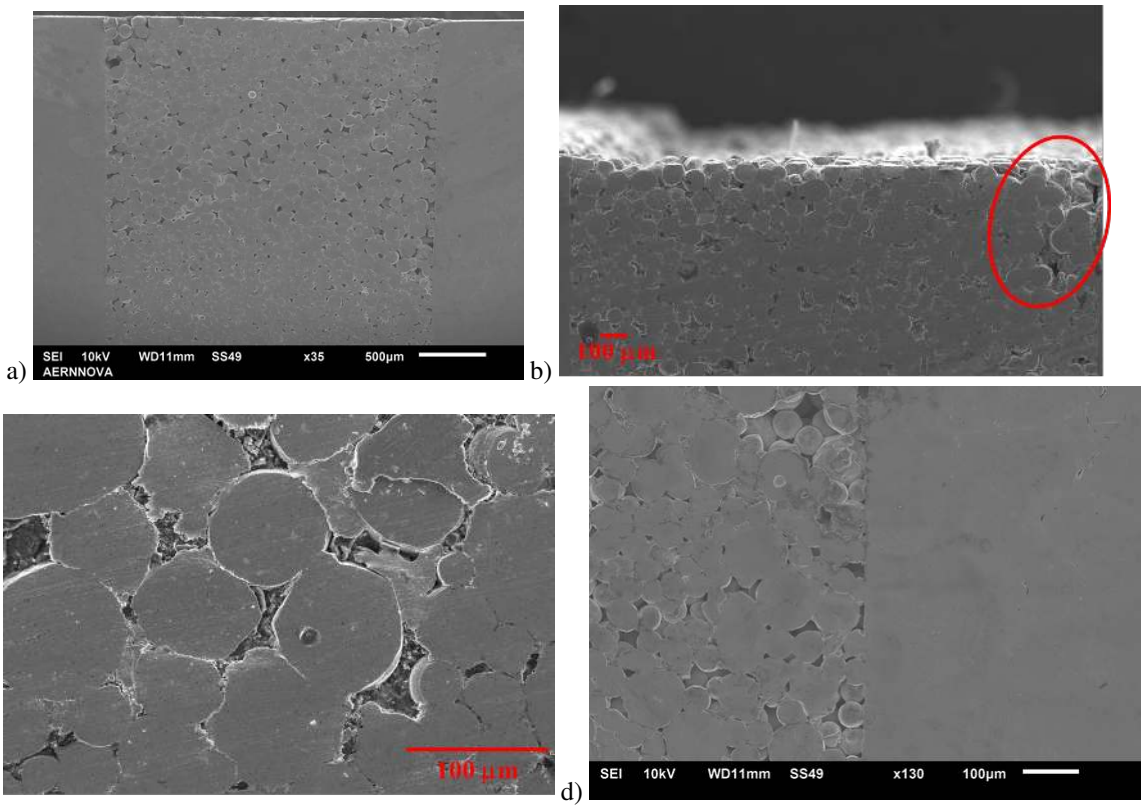

Fig. 6. Micrographs of the inner surface of the groove filled with larger particles (40-63 μm) after sintering at 1050°C, (a) whole groove surface, (b) upper profile, (c) particles at the middle of the groove and (d) sintered particles at the wall's groove.

This was 4 times larger than the one observed for the same kind of particles sintered at 1000°C. Because of the larger shrinkage, we observed the creation of larger defects all around the crack. In this case, delamination between the particle and the wall is presented not only at the surface, but also close to the bottom of the samples. In the middle of the groove, we observe larger pores than those observed for the sample filled with the same particle distribution but sintered at 1000°C. This observation could be an indicator showing that defects could not only be created in the weaker necks developed between the flat surface of the wall and particles because of the stronger strain generated by the constrained sintering of the powders, but also shows that the stronger necks developed between particle-particle could be breaking down as well as the weaker ones as observed in Figure 7c. The joint at the surface of the wall's groove seems to be affected by the larger shrinkage experimented by the smaller particles at higher sintering temperatures, and the necks developed during the sintering are smaller than those created between particles. That might be due to the shorter time of contact between the flat surface and the particles because the shrinkage forces make them to migrate to the center of the sample, causing the smaller necks developed at the surface to break, as we can observe in Figure 7d. That causes a higher relative density at the center of the groove than close to the walls.

In particular sintering of powders is a densification process that reduces its volume by pulling away the remaining porosity. During that process, indentation between contacting particles causes attraction forces, making that the mass of powders (during free sintering) undergoes compression stresses, which pull the particles toward the center of the sample. On the other hand, for constrained sintering, particles attached to the wall undergo tension stresses and particles at the center of the groove undergo compression stresses. Those stresses are stronger as densification is higher, which in our case, it is produced by smaller particles as it was found in Figure 3.

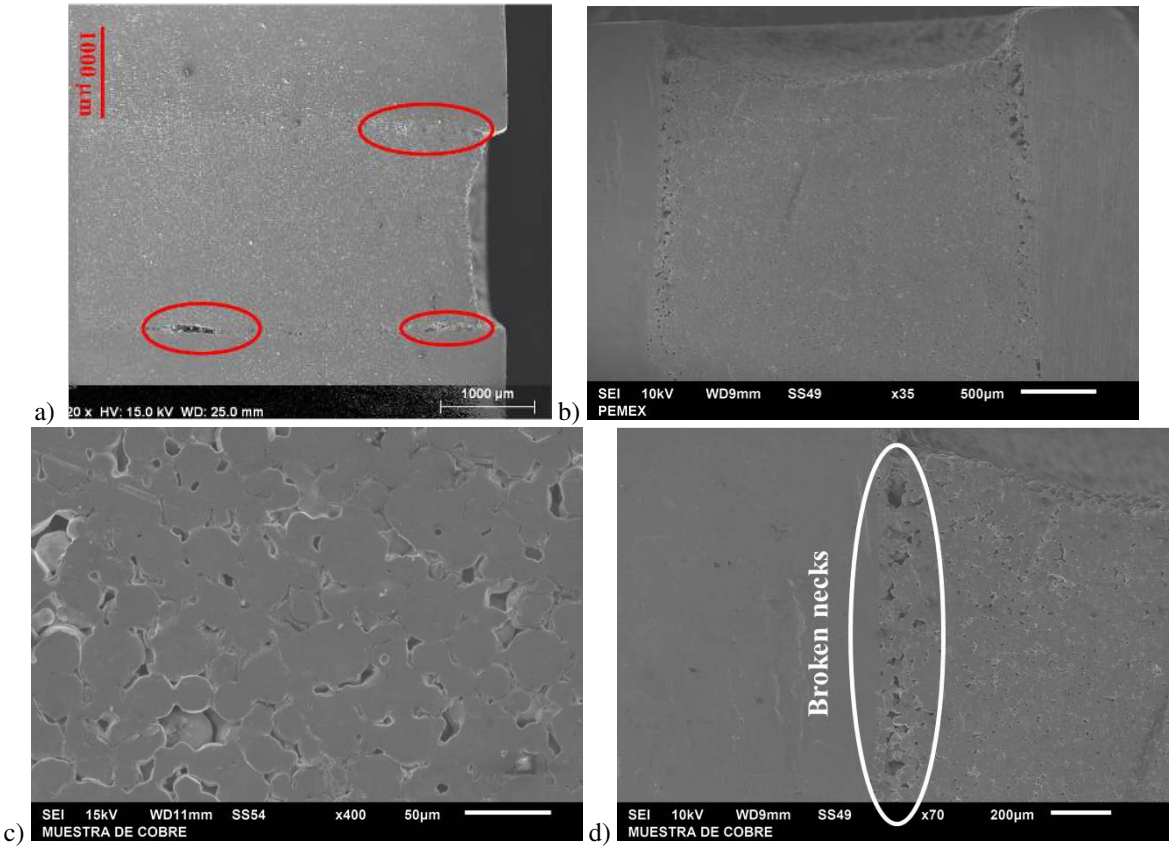

Fig. 7. Micrographs of the inner surface of the groove filled with larger particles (40-63 μm) after sintering at 1050°C, (a) whole groove surface, (b) upper profile, (c) particles at the middle of the groove and (d) sintered particles at the wall's groove.

It was expected that larger densification should cause the creation of defects close to the surface and the walls. Nevertheless, we also found that defects can be generated far from the surface, and that stresses generated by the densification forces are able to break down the contacts already developed between particle-particle at the middle of the sample, in spite of compression stresses that would help to densify the powders. Those defects might be produced by non-homogeneous initial packing, or initial defect that can be easily growth because of the sintering stresses during the thermal cycle. When densification increases the first defects are created on the weaker joint between particle-wall, since the diffusion between a flat and curved surfaces is lower than between two curved surfaces, however those defects appear only for smaller particles, which means that only higher densification is able to produce enough tension to break down that joint. Further, defects are not exclusive at the surface but also close to the bottom. Those results are consistent with the ones observed by Martin *et al*, (2009) in numerical simulations of constrained sintering and defects propagation.

On the other hand, it was observed that larger particles provided a better distribution of particles in the groove and the sintering between particle and wall were well developed. As the densification is smaller for this kind of particles, no defects were created. However, there was still higher pore fraction inside the groove because of the lower densification. The remaining pores seem to be larger than those observed for the smaller particles from the SEM images. Although these observations should be taken carefully because during the polishing step, the surface is smeared therefore pores are artificially filled.

Conclusions

Constrained sintering of powders has been evaluated by filling grooves created artificially with powders.

The effect of both, sintering temperature and the particle size distribution, on the evolution of the inner microstructure was investigated. It was demonstrated that particles could be used to repair fissures because particles were well sintered on the wall's surface for both particle size distributions used in this paper even if the larger densification causes delamination of the particles from the wall.

It was assessed that defects created during sintering are due to the higher tensile stresses generated at the joint between walls and particles by the densification process which is larger when higher temperature and smaller particles are used. It was also demonstrated that developed necks between particles or particle-wall could be breaking as the internal stresses increase by enhancing the densification of the powders.

We conclude that higher densification is detrimental in constrained sintering since defects like delamination between powders and walls might cause that the joint between powders and the solid part is weaker, therefore the mechanical properties will be reduced. In consequence we suggest that for repairing fissures, larger particles or lower temperatures are more appropriated.

Acknowledgements

The authors would like to thank to CONACyT and the Scientific Research Department of the UMSNH for the financial support and the facilities to develop this study.

References

Anselmi-Tamburini U, Garay JE, Munir ZA. (2006). Fast low-temperature consolidation of bulk nanometric ceramic materials. *Scripta Materialia 54*, 823-828.

Ch'ng HN, Pan J. (2007). Sintering of particles of different sizes. *Acta Materialia 55* 813-824.

Coble R.L. (1958). Initial sintering of alumina and hematite. *Journal of American Ceramic Society 41*, 55-62.

Exner H. (1979). Principles of single phase sintering. *Reviews on Powder Metallurgy and Physical Ceramics 1*, 7-251.

Exner HE, Petzow G. (2006). A critical assessment of porosity coarsening during solid state sintering. *Advances in Science and Technology 45*, 539-548.

Frenkel J. (1945) Viscous flow of crystalline bodies under the action of surface tension, *Journal of Physics* (Moscow).

German R.M. (1978). Surface area reduction kinetics during intermediate stage sintering. *Journal of American Ceramic Society 61*, 272-274.

Henrich B, Wonisch A, Kraft T, Moseler M, Riedel H. (2007). Simulations of the influence of rearrangement during sintering. *Acta Materialia 55*, 753-762.

Hsueh C.H. (1985).Sintering of a Ceramic Film on a Rigid Substrate. *Scripta Metallurgica 19*, 1213-1217.

Khalil A.K., Abdulhakim A.A. (2012). Effect of high-frequency induction heat sintering conditions on the microstructure and mechanical properties of nanostructured magnesium/hydroxyapatite nanocomposites. *Materials and Design 36*, 58-68.

Kingery WD, Berg M. (1955). Study of the initial stages of sintering solids by viscous flow, evaporation-condensation and self-diffusion. *Journal of Applied Physics 26*, 1205-1212.

Kuczynski GC. (1949). Self-diffusion in sintering of metallic particles. *Transactions of the American Institute of Mining and Metallurgical Engineers 185*, 169-178.

Lame O, Bellet D, Di Michiel M, Bouvard D. (2004). Bulk observation of metal powder sintering by X-ray synchrotron microtomography. *Acta Materialia 52*, 977-984.

Martin CL, Bordia RK. (2009). The effect of a substrate on the sintering of constrained sintering. *Acta Materialia 57*, 549-558.

Martin CL, Camacho-Montes H, Olmos L, Bouvard D, Bordia RK. (2009). Evolution of defects during sintering-discrete element simulations. *Journal of American Ceramic Society 92*, 1435-1441.

Martin CL, Schneider LCR, Olmos L, Bouvard D. (2006). Discrete element modeling of metallic powder sintering. *Scripta Materialia 55*, 425 - 428.

Mori K, Matsubara H, Noguchi N. (2004). Micro-macro simulation of sintering process by coupling Monte Carlo and finite element methods. *International Journal of Mechanical Sciences 46*, 841-854.

Mori K, Ohashi M, Osakada K. (1998).Simulation of microscopic shrinkage behavior in sintering of powder compact. *International Journal of Mechanical Sciences 40*, 989-999.

Olmos L, Martin CL, Bouvard D, Bellet D, Di Michiel M. (2009). Investigation of the sintering of heterogeneous powder systems by synchrotron microtomography and discrete element simulation. *Journal of American Ceramic Society 92*, 1492-1499.

Olmos L, Martin CL, Bouvard D. (2009). Sintering of mixtures of powders: experiments and modeling. *Powder Technology 190*, 134-140.

Olmos L, Takahashi T, Bouvard D, Martin CL, Salvo L, Bellet D, Di Michiel M. (2009) Analysing the sintering of heterogeneous powder structures by *in situ* microtomography. *Philosophical Magazine 89*, 2949-2965.

Pan J, Le H, Kucherenko S, Yeomans JA. (1998). A model for the sintering of spherical particles of different sizes by solid state diffusion. *Acta Materialia 46*, 4671-4690.

Panigrahi BB, Godkhindi MM, Das K, Mukunda PG, Ramakrishnan P. (2005). Sintering kinetics of micrometric titanium powder. *Materials Science and Engineering A A396*, 255-262.

Parhami F, McMeeking RM. (1998). A network model for initial stage sintering. *Mechanics of Materials 27*, 111-124.

Rasp T, Jamin C, Wonisch A, Kraft T, Guillon O. (2012). Shape Distortion and Delamination During Constrained Sintering of Ceramic Stripes: Discrete Element Simulations and Experiments. *Journal of American Ceramic Society 95*, 586-592.

Scherer GW, Garino T. (1985). Viscous Sintering on a Rigid Substrate. *Journal of American Ceramic Society 68*, 216-220.

Showaiter N, Youseffi M. (2008). Compaction, sintering and mechanical properties of elemental 6061 Al powder with and without sintering aids. *Materials and Design 29*, 752-762.

Subrata K.G. Partha S. (2011). Crack and wear behavior of SiC particulate reinforced aluminium based metal matrix composite fabricated by direct metal laser sintering process. *Materials and Design 32*, 139-145.

Tikare V, Braginsky M, Bouvard D, Vagnon A. (2006). An Experimental Validation of a 3D Kinetic, Monte Carlo Model for Microstructural Evolution during Sintering. *Advances in Science and Technology 45*, 522-529.

Upadhyaya A, German RM. (1998). Densification and dilatation of sintered W-Cu alloys. *International Journal of Powder Metallurgy 34*, 43-55.

Vagnon A, Rivière JP, Missiaen JM, Bellet D, Di Michiel M, Josserond C, Bouvard D. (2008). 3D statistical analysis of a copper powder sintering observed in situ by synchrotron microtomography. *Acta Materialia 56*, 1084-1096.

Wei Z, Yong T, Bin L, Rong S, Lelun J, Hui KS, Hui KN, Haimin Y. (2012). Compressive properties of porous metal fiber sintered sheet produced by solid-state sintering process. *Materials and Design 36*, 414-418.